High-Throughput Preparation of Monodispersed Layered Double Hydroxides via Microreaction Technology

Mingyue Ren[1,2], Mei Yang[1], Guangwen Chen[1]* and Quan Yuan[1]

[1]*Dalian National Laboratory for Clean Energy, Dalian Institute of Chemical Physics, Chinese Academy of Sciences, 457 Zhongshan Road, Dalian 116023, China*
[2]*University of Chinese Academy of Sciences, Beijing 100049, China*

Received: 26 April 2014; accepted: 21 June 2014

A facile and reproducible method based on microreaction technology has been developed for the continuous preparation of layered double hydroxides (LDHs) with narrow particle size distribution. Mg–Al–CO_3, Mg–Al–NO_3, Mg–Al–Cl, and other different kinds of LDHs containing binary, ternary, and quadruple metal cations were successfully prepared. Due to the enhanced mixing, a high slurry throughput of 300 mL/min in a single reaction channel was obtained.

Keywords: layered double hydroxides, microchannel reactor, particle size distribution

1. Introduction

Layered double hydroxides (LDHs), also known as hydrotalcite-like compounds, are an extensive class of synthetic anionic clays. The general formula of LDHs may be described as $[M^{2+}_{1-x}M^{3+}_{x}(OH)_2]^{x+}(A^{n-}_{x/n})\cdot mH_2O$, where M^{2+} and M^{3+} are divalent and trivalent metal cations which occupy octahedral holes in a brucite-like layer, and A^{n-} can be various kinds of inorganic or organic anion which is located in the hydrated interlayer galleries [1]. Due to the special layered structure and high anion exchange behavior, LDHs have been widely used as functional materials [2], including ion exchange hosts [3], catalysts or catalyst supports [4], flame retardants [5], adsorbents [6], biomedical materials [7], luminescent materials [8], and magnetic materials [9]. Conventionally, LDHs are synthesized by coprecipitation method at constant or variable pH in batch reactor [10]. This process generally involves nucleation, growth, agglomeration, and aging stages, which are significantly influenced by the process parameters such as stirring rate, residence time, reaction temperature, etc. Therefore, it is very necessary to ensure a good control of process parameters to obtain LDHs with good quality. However, as is well known, it is difficult for conventional process to offer a uniform precipitation condition. Firstly, there is always a gradient of supersaturation due to the limitation of mixing and heat transfer in batch reactor, which affects the nucleation and growth stages dramatically. Secondly, because of intermittent operation mode, the residence time of precipitate particles markedly varies from the beginning to the end of precipitation process, which inevitably leads to a wide particle size distribution and poor reproducibility. Furthermore, considering the scale-up effect of batch reactor, whether the result in a lab can be replicated or not on a mass production is still a problem.

To overcome the disadvantages of conventional process, as noted above, several novel approaches have been proposed in recent years. Duan et al. put forward a new method for preparing LDHs nanomaterials with a uniform crystal size, which involved a rapid mixing with nucleation process in a colloid mill and a separate aging process after that [11]. Afterwards, Abelló et al. invented a mixing enhancement in-line dispersion–precipitation method for the preparation of LDHs. The novel process was accomplished in a continuous mode by using a vigorously stirred microreactor with in-line pH control [12]. More recent studies by Wang et al. demonstrated a continuous-flow supercritical hydrothermal method for the synthesis of LDHs nanoplates using a nozzle reactor [13]. Evidently, all these novel approaches were in semi-continuous or continuous operation and dedicated to mixing intensification. However, the high energy consumption and scale-up difficulties of these approaches can not be neglected. To avoid these issues, some researchers paid their attention to microreaction technology. So far, microreactors have been widely used in many fields due to its high heat and mass transfer rate, large surface-to-volume ratio, and many other virtues resulting from its characteristic scale of submillimeter size [14]. Shirure et al. reported a narrow channel reactor for the preparation of LDHs, which showed better results in terms of particle size and power consumption compared with a conventional stirred batch reactor [15]. However, the particle size was above 10 μm with obvious agglomeration problem. Pang et al. reported a simple method for the synthesis of naked Mg_2Al–NO_3 LDH nanosheets without organic substitutes in a T-type microchannel reactor [16], and this process was only for the preparation of LDH nanosheets but did not involve the preparation of plate-like LDHs.

In the present work, we focus on the high-throughput preparation of monodispersed LDHs with narrow particle size distribution based on microreaction technology. To this end, a continuous-flow T-type microchannel reactor with a special outlet structure was fabricated and the reaction process was conducted at relatively high Reynolds number. Depending on these conditions, different kinds of LDHs containing binary, ternary, and quadruple metal cations were successfully prepared. Particularly, Mg–Al–NO_3 and Mg–Al–Cl LDHs were synthesized successfully in the condition without inert gas protection.

2. Results and Discussion

The continuous-flow system for preparing LDHs is assembled as shown in Figure 1, and the constructions of microchannel reactor and T-shape microchannel plate are shown in Supporting Information. The microchannel reactor was composed of two microchannel plates which were sealed with two stainless steel plates. The microchannel plates were fabricated with polyarylsulfone (PASF), which was resistant to corrosion and high temperature. The size of two inlet channels and one reaction channel was 800 μm (width)×800 μm (depth)×10 mm (length) with a rectangular cross section. The

* Author for correspondence: gwchen@dicp.ac.cn

DOI: 10.1556/JFC-D-14-00014

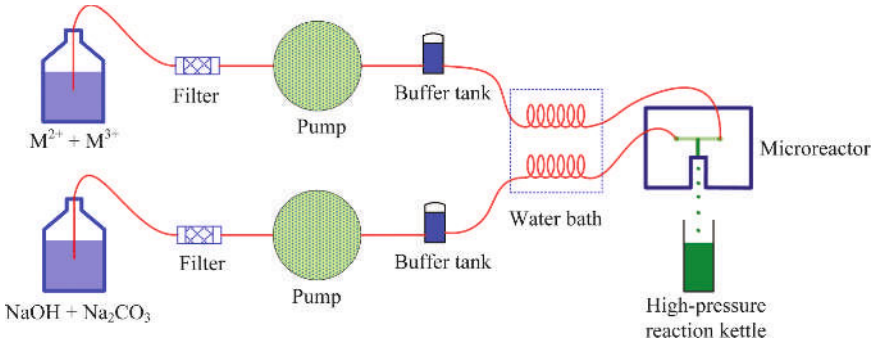

Figure 1. The experimental setup of preparing LDHs

outlet at the end of the reaction channel was designed without any turnings in order to decrease the pressure drop along the whole reactor and prevent the reactor from blockage.

In a typical process, the flow velocity in the reaction channel was up to 7.8 m/s, which contributed to a total flow rate of ca. 18 L/h and Reynolds number up to 6200 when using water as a carrier medium. It was evident that the precipitation process was carried out at turbulent flow, and the theoretical mixing time was about 0.5 ms in an ideal situation at this Reynolds number according to the previous report [17], indicating a high efficient micromixing of reactants. The residence time of reactants was as short as 1.3 ms in the reaction channel. This short residence time offered an opportunity to physically separate the nucleation of LDHs from their aging process, and thus made a narrow particle size distribution possible. Figure 2 shows the X-ray diffraction (XRD) patterns of the prepared $Mg_3Al–CO_3$ LDHs. As expected, the sample without aging exhibited hydrotalcite as the only crystalline phase with the smallest crystalline size of 5 nm according to Scherrer's equation, indicating that the nucleation of $Mg_3Al–CO_3$ was extraordinarily fast. To obtain a better crystallinity, hydrothermal treatment was employed. All reflections of the samples with hydrothermal treatment in less than 3 h at 150 °C can be assigned to hydrotalcite; meanwhile, the intensities of reflection peaks increased with the increase of hydrothermal time. However, accompanied by further extension of hydrothermal time from 3 h to 8 h, impurity phase of magnesium carbonate appeared, implying that $Mg_3Al–CO_3$ LDH started to decompose. The same phenomenon was found at 180 °C for 3 h, but no decomposition was observed at 100 °C for 8 h. This indicated that hydrothermal temperature and time were both crucial and should be controlled within a certain range to ensure a pure phase. In addition, the stability of LDHs was also influenced by the molar ratio of Mg^{2+} to Al^{3+}. As shown in Supporting Information, $Mg_4Al–CO_3$ and $Mg_2Al–CO_3$ started to decompose at 150 °C in the range of 2–3 h and less than 1 h, respectively. Both were less stable in comparison with $Mg_3Al–CO_3$.

Figure 3 shows the particle size distribution of $Mg_3Al–CO_3$ LDHs hydrothermally treated at 150 °C for 0–2 h. It can be seen that the particle size was about 100–1000 nm when the temperature just rose to 150 °C, for the initially formed particles were extremly small and easily agglomerated due to the high surface energy. As the hydrothermal time increased from 0 h to 0.5 h, the particle size decreased rapidly to 30–80 nm; meanwhile, the particle size distribution became quite narrow. After that, the particle size increased slowly to 30–110 nm with the increase of hydrothermal time from 0.5 h to 2 h, and the particle size distribution became a little broader. This may be explained by the dissolution–recrystallization process [18]. More specifically, as the temperature increased, the small particles started to dissolve into the solution and gradually grew into big LDHs nanoparticles with high crystallinity.

To visually observe the particle size distribution of LDHs, transmission electron microscopy (TEM) was performed. Figure 4 presents the TEM images of LDHs nanoparticles hydrothermally treated at 150 °C with different Mg^{2+}/Al^{3+} ratios. Clearly, the particles were monodispersed and all exhibited better hexagonal platelike morphology with the increasing hydrothermal time. Although there was some decomposition, the particles grew from ca. 40–100 nm to 50–150 nm for $Mg_2Al–CO_3$ with regular hexagonal platelike. For $Mg_3Al–CO_3$, the particle size went up from ca. 20–100 nm to 30–150 nm, which was in accordance with the results obtained on laser particle size analyzer. Unlike the former two, $Mg_4Al–CO_3$ switched from amorphous aggregation to fragmented pieces with the size of ca. 20–80 nm. Taking the TEM images and laser particle size analyzer results together, we observed that the products prepared by microreaction technology were, as expected, with narrow particle size distribution and regular

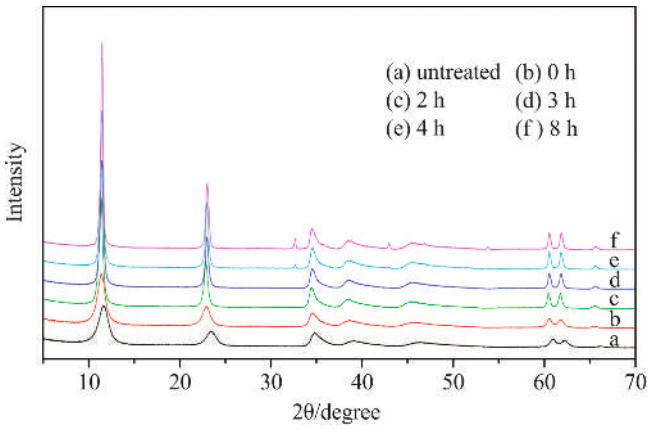

Figure 2. XRD of $Mg_3Al–CO_3$ LDHs hydrothermally treated at 150 °C

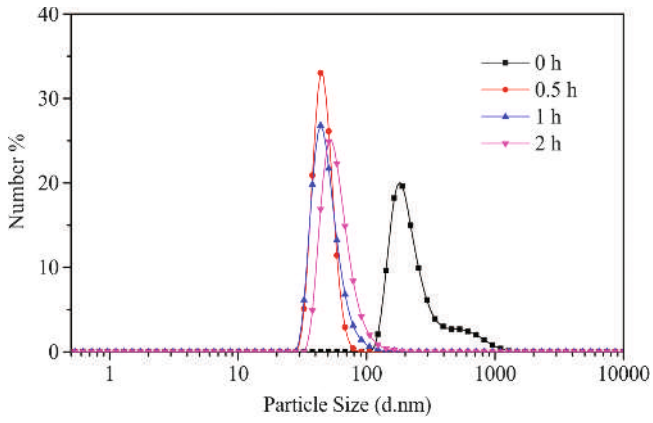

Figure 3. Particle size distribution of $Mg_3Al–CO_3$ LDHs hydrothermally treated at 150 °C

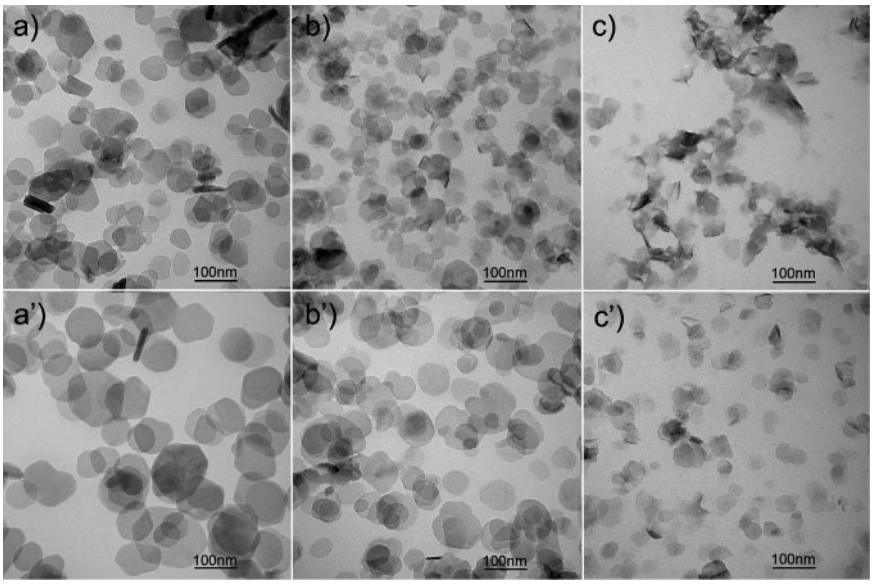

Figure 4. TEM images of LDHs hydrothermally treated at 150 °C for 1 h: a) $Mg_2Al–CO_3$, b) $Mg_3Al–CO_3$, and c) $Mg_4Al–CO_3$ and 2 h: a′) $Mg_2Al–CO_3$, b′) $Mg_3Al–CO_3$, and c′) $Mg_4Al–CO_3$

particle shape, which might be because the initially formed particles were more uniform in microchannel reactor.

As mentioned above, LDHs and their derivatives can be widely used as functional materials owing to various kinds of cations/anions and different combinations of metal cations. To demonstrate the universality and flexibility of the method in this study, other different kinds of LDHs containing binary, ternary, and quadruple metal cations with CO_3^{2-} as anion were successfully prepared, such as $Mg_3Fe–CO_3$, $Ni_3Al–CO_3$, $Mg_6AlFe–CO_3$, $Mg_3Zn_3Al_2–CO_3$, and $CuCoZnAl–CO_3$, as shown in the XRD patterns (Supporting Information). TEM images of LDHs containing four kinds of metal cations were shown in Figure 5, and the $\Sigma n(M^{2+})/\Sigma n(M^{3+})$ was 3/1 for all the six kinds of LDHs nanoparticles.

Besides CO_3^{2-}, LDHs with anions of NO_3^-, Cl^- or SO_4^{2-} are usually synthesized and used as precursors for their weak anion exchange ability. In the conventional process, since CO_3^{2-} owns distinctive ion exchange ability, these LDHs should be prepared with inert gas protection to avoid contamination of CO_2 in the air over a long reaction time. Inherently, microchannel reactor can offer an enclosed reaction space and extremely short residence time, which are both beneficial for preparation of NO_3^-, Cl^-, and SO_4^{2-} LDHs. In this work, $Mg_3Al–NO_3$ and $Mg_3Al–Cl$ LDHs were synthesized successfully in the condition without inert gas protection, as shown in Supporting Information. Unfortunately, $Mg_3Al–SO_4$ LDH was not obtained in the same condition no matter without any treatment or aging at 100 °C for 4 h. The relevant study is currently under way.

In conclusion, LDHs with narrow particle size distribution and good reproducibility were successfully prepared in a continuous-flow microchannel reactor with high slurry throughput of 300 mL/min in a single reaction channel. Not only different kinds of LDHs containing binary, ternary, and quadruple metal cations with CO_3^{2-} as anion but also $Mg_3Al–NO_3$ and $Mg_3Al–Cl$ LDHs in the condition without inert gas protection were successfully synthesized. Our work has demonstrated that microchannel reactor can generate a stable and homogeneous chemical environment for LDHs preparation due to high mass and heat transfer. It can readily deal with scale-up to meet industrial

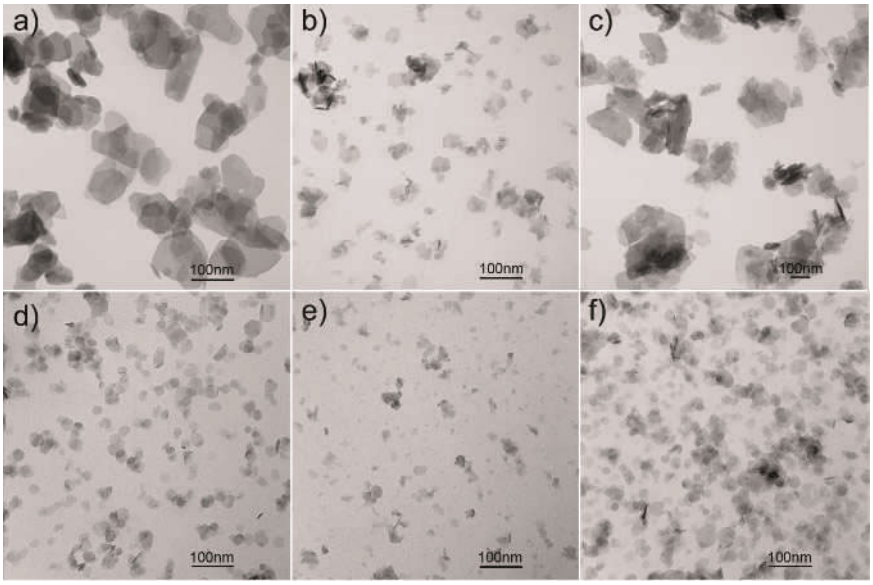

Figure 5. TEM images of LDHs nanoparticles containing four kinds of metal cations with CO_3^{2-} as the anion: a) Cu:Co:Zn:Al=1:1:1:1; b) Cu:Co:Zn:Cr=1:1:1:1; c) Cu:Zn:Al:Cr=3:3:1:1; d) Mg:Ni:Fe:Al=3:3:1:1; e) Mg:Cu:Ni:Al=1:1:1:1; and f) Mg:Co:Ni:Al=1:1:1:1

requirement by increasing the number of microchannels. Considering the miniaturized characteristic and high energy efficiency, the approach developed in this study can serve as a potential method for the industrial production of LDHs, and probably for other nanomaterials.

3. Experimental

3.1. Materials. Sodium hydroxide, sodium carbonate, magnesium nitrate, aluminum nitrate, ferric nitrate, nickel nitrate, copper nitrate, cobalt nitrate, magnesium chloride, aluminum chloride, magnesium sulfate, and aluminum sulfate were obtained from Kemiou Chemical Reagent Co. (Tianjin, China). Zinc nitrate and chromium nitrate were purchased from Sinopharm Chemical Reagent Co. (Shanghai, China). All chemicals were analytically pure and used without further purification.

3.2. Synthesis of LDHs Contained CO_3^{2-}. In the present work, the LDHs were prepared by the precipitation process in a T-type microchannel reactor and followed by aging or hydrothermal process. In a typical synthesis process of LDHs, divalent and trivalent metal cations were dissolved in the deionized water as solution A; meanwhile, NaOH and Na_2CO_3 were dissolved in the deionized water as solution B. The total molar concentration of metal caions in solution A was 0.50 mol/L, and the molar concentration ratio of divalent metal cations to trivalent was 2/1, 3/1, or 4/1. The concentrations of the base in solution B were controlled to maintain the pH of the slurry at a selected value as follows: $[NaOH]=1.6([M^{2+}]+[M^{3+}])$, $[NaCO_3]=2.0[M^{3+}]$. With the same volume flow rate of 150 mL/min, solution A and B were pumped first through water bath to preheat and then into the microchannel reactor. The reaction was conducted at 80 °C. One part of the obtained slurry was washed with deionized water thoroughly and dried at 80 °C for 8 h in air (untreated), and the other part was treated by the aging or hydrothermal process at 100–180 °C for 0–8 h in a Teflon-lined stainless steel autoclave of 100 mL capacity (the 0 h means that the tempreture of slurry in the autoclave rises to 150 °C and keeps for 0 h). The autoclave was fixed on the arm of axle in the oven and rotated 60 rounds per minute for stirring. After naturally cooling down to room temperature, the slurry was centrifuged and thoroughly washed with deionized water and then dried at 80 °C for 8 h in air. There was no clogging problem observed during the preparation of LDHs in this work. The subscript number in the sample name such as $Mg_3Al–CO_3$ represents the relative molar ratio of metal cations employed in the synthesis mixture.

3.3. Synthesis of LDHs Contained no CO_3^{2-}. Carbon dioxide-free water was prepared by boiling the deionized water for 10 min and then cooled for the solution preparation and product washing. The Mg^{2+} (0.50 mol/L) and Al^{3+} (0.17 mol/L) were dissolved in the deionized water as solution A; meanwhile, NaOH (1.00 mol/L) was dissolved in the deionized water as solution B. The rest of the procedure was the same as the synthesis of LDHs contained CO_3^{2-}, except the aging part treated at 100 °C for 4 h and the drying part carried out in a vacuum oven. The whole process was without inert gas protection.

3.4. Characterization Techniques. X-ray diffraction (XRD) analysis was carried out on a PANalytical X'Pert-Pro powder X-ray diffractometer using Cu Kα radiation (λ=0.1541 nm, 40 kV, and 40 mA) with a scanning rate of 10° min^{-1}. Particle size distributions were obtained on a Malvern Zetasizer Nano 90 laser particle size analyzer by means of dynamic light scattering with the ethanol as dispersant, and the size distribution by number was calculated by Mie theory based on intensity distribution. Transmission electron microscope (TEM) images were obtained on a JEOL JEM-2000EX with the accelerating voltage of 120 kV. The powder sample was dispersed in ethanol and with a sonic bath for 10 min before mounted onto a carbon-coated copper grid for the test.

Acknowledgment. We gratefully acknowledge the financial support for this project from the National Natural Science Foundation of China (Nos. 21225627, 21106141, and 91334201).

Supporting Information

Electronic Supplementary Material (ESM) is available in the online version at doi: 10.1556/JFC-D-14-00014.

References

1. (a) Cavani, F.; Trifiro, F.; Vaccari, A. *Catal. Today* **1991**, *11*, 173–301; (b) Rives, V. *Layered Double Hydroxides: Present and Future*; Nova Science Publishers: New York, 2001; (c) Auerbach, S. M.; Carrado, K. A.; Dutta, P. K. *Handbook of Layered Materials*, Taylor & Francis: New York, 2004.

2. (a) Li, F.; Duan, X. *Struct. Bonding (Berlin)* **2006**, *119*, 193–223; (b) Evans, D. G.; Duan, X. *Chem. Commun.* **2006**, *5*, 485–496.

3. (a) Khan, A. I.; Ragavan, A.; Fong, B.; Markland, C.; O'Brien, M.; Dunbar, T. G.; Williams, G. R.; O'Hare, D. *Ind. Eng. Chem. Res.* **2009**, *48*, 10196–10205; (b) Rives, V.; Ulibarri, M. A. *Coord. Chem. Rev.* **1999**, *181*, 61–120.

4. (a) Xu, Z. P.; Zhang, J.; Adebajo, M. O.; Zhang, H.; Zhou, C. *Appl. Clay Sci.* **2011**, *53*, 139–150; (b) Sels, B.; Vos, D. D.; Buntinx, M.; Pierard, F.; Mesmaeker, A. K.-D.; Jacobs, P. *Nature* **1999**, *400*, 855–857; (c) Turco, M.; Bagnasco, G.; Costantino, U.; Marmottini, F.; Montanari, T.; Ramis, G.; Busca, G. *J. Catal.* **2004**, *228*, 43–55.

5. (a) Wang, Z.; Han, E.; Ke, W. *Prog. Org. Coat.* **2005**, *53*, 29–37; (b) Nyambo, C.; Songtipya, P.; Manias, E.; Jimenez-Gasco, M. M.; Wilkie, C. A. *J. Mater. Chem.* **2008**, *18*, 4827–4838.

6. Goh, K. H.; Lim, T. T.; Dong, Z. *Water Res.* **2008**, *42*, 1343–1368.

7. Xu, Z. P.; Zeng, Q. H.; Lu, G. Q.; Yu, A. B. *Chem. Eng. Sci.* **2006**, *61*, 1027–1040.

8. Yan, D.; Lu, J.; Ma, J.; Qin, S.; Wei, M.; Evans, D. G.; Duan, X. *Angew. Chem., Int. Ed.* **2011**, *50*, 7037–7040.

9. Coronado, E.; Marti-Gastaldo, C.; Navarro-Moratalla, E.; Ribera, A.; Blundell, S. J.; Baker, P. J. *Nat. Chem.* **2010**, *2*, 1031–1036.

10. He, J.; Wei, M.; Li, B.; Kang, Y.; Evans, D. G.; Duan, X. *Struct. Bonding (Berlin)* **2006**, *119*, 89–119.

11. Zhao, Y.; Li, F.; Zhang, R.; Evans, D. G.; Duan, X. *Chem. Mater.* **2002**, *14*, 4286–4291.

12. Abelló, S.; Pérez-Ramírez, J. *Adv. Mater.* **2006**, *18*, 2436–2439.

13. Wang, Q.; Tang, S. V.; Lester, E.; O'Hare, D. *Nanoscale* **2013**, *5*, 114–117.

14. (a) Dietrich, T. R. *Microchemical Engineering in Practice*; John Wiley & Sons Ltd.: Hoboken, 2009; (b) Yang, M.; Men, Y.; Li, S.; Chen, G. *Appl. Catal., A* **2012**, *433–434*, 26–34; (c) Yang, M.; Li, S.; Chen, G. *Appl. Catal., B* **2011**, *101*, 409–416; (d) Chen, Y.; Su, Y.; Jiao, F.; Chen, G. *RSC Adv.* **2012**, *2*, 5637–5644; (e) Zhao, Y.; Yao, C.; Chen, G.; Yuan, Q. *Green Chem.* **2013**, *15*, 446–452.

15. Shirure, V. S.; Nikhade, B. P.; Pangarkar, V. G. *Ind. Eng. Chem. Res.* **2007**, *46*, 3086–3094.

16. Pang, X.; Sun, M.; Ma, X.; Hou, W. *J. Solid State Chem.* **2014**, *210*, 111–115.

17. (a) Ying, Y.; Chen, G.; Zhao, Y.; Li, S.; Yuan, Q. *Chem. Eng. J.* **2008**, *135*, 209–215; (b) Falk, L.; Commenge, J. M. *Chem. Eng. Sci.* **2010**, *65*, 405–411; (c) Kumar, V.; Paraschivoiu, M.; Nigam, K. D. P. *Chem. Eng. Sci.* **2011**, *66*, 1329–1373.

18. Xi, G.; Xiong, K.; Zhao, Q.; Zhang, R.; Zhang, H.; Qian, Y. *Cryst. Growth Des.* **2006**, *6*, 577–582.